Characterization of the L_6D_6 detector

Yuta Sato

August 31, 2016

1 Introduction

The cross sections of nuclear reactions are derived from both experimental data and theoretical predictions, so it's necessary to perform new and more accurate measurements of many isotopes and reactions.

The n_TOF facility at CERN is in the field of neutron-induced cross section measurements. These reactions are of fundamental importance for the study of nuclear structure and of the mechanism of fission reactions. To measure the cross sections of the neutron-induced reactions (n, γ), we want to detect only γ-ray.

Among them, neutron capture reactions play an important role both for stellar nucleosynthesis and nuclear reactor calculations. To detect the γ-rays coming from the (n, γ) reactions, one of the technique exploited at the n_TOF uses an array of four liquid scintillator. Since the main background for these reactions comes from γ-ray produced at a second time by scattered neutrons, the choice of the material is very important in order to minimize it. As scintillation liquid the deuterated benzene (C_6D_6) is chosen, being a very fast, hydrogen-free scintillator. Moreover, both the liquid and the photomultiplier are contained in a carbon-fiber case, since C has a very low neutron-capture cross-section.

A brand new concept of detector has been recently introduced at n_TOF[1], called L_6D_6, an my work as a Summer Student is to calibrate the relation between the deposited energy and the pulse height of the signals from the detector L_6D_6 filled with C_6D_6.

2 Detection Set-Up

2.1 Detector preparation

As a first step, I filled two detectors, named $L_6D_6 - F$ and $L_6D_6 - G$, with the liquid scintillator C_6D_6. Figure 1 shows the external carbonfiber case: the bottom part is a container for the scintillation liquid C_6D_6, while the photomultiplier with its voltage divider are contained in the upper part. The small volume on the top left of the figure is an expansion volume, needed to let air flow from the main tank if the detector position is different from the vertical one.

2.2 First analysis

After the filling operation, I have collected a set of data with ^{137}Cs and ^{88}Y sources, using a multichannel analyzer (MCA). In this way, the correct behaviour of the L_6D_6 can be checked. Each measurement has been carried out for a 5 minutes time window.

Figure 1: L_6D_6 detector filled with C_6D_6 liquid scintillator.

Figure 2 shows the histogram obtained from MCA. From this result, we can see the Compton edge for each source, detectors are working well. We confirmed that these peaks are the Compton edge by changing the gain of the amplifier.

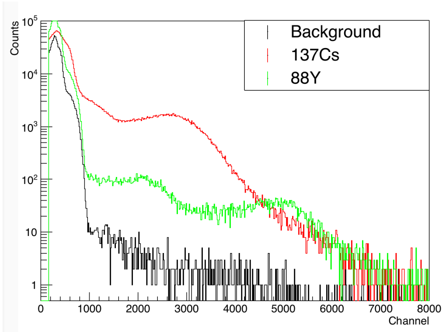

Figure 2: Raw data obtained by detector G.

2.3 Average pulse shape

I put ^{137}Cs and ^{88}Y in front of the detector, and recorded approximately 300 pulses for each source. Threshold was chosen not to trigger the noise. The parameters for each run are shown in Table 1.

Source	Threshold [mV]	Horizontal axis [ns/div]	Vertical axis [mV/div]	Number of pulses collected	Color of each plot in Figure 3 (b)
^{137}Cs	-15.0	10	10	329	Yellow
^{88}Y	-60.0	10	100	304	Black
^{88}Y	-60.0	10	20	307	Red
^{88}Y	-150	10	100	329	Green
^{88}Y	-150	10	500	303	Blue

Table 1: Parameters of the oscilloscope for each run

Figure 3 is an example of the pulse shapes. The black line corresponds to each signal. I calculated an average pulse shape from these signals. The average one is expressed in a red line.

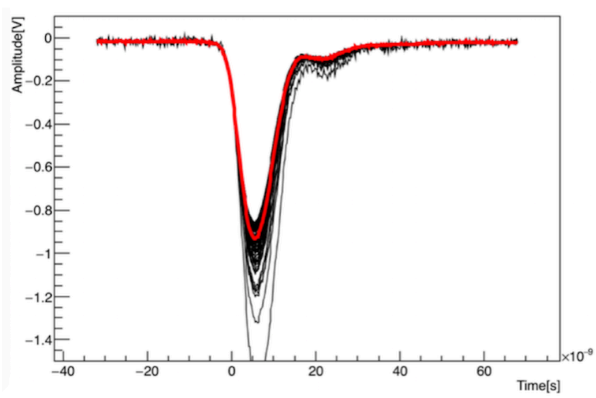

(a)

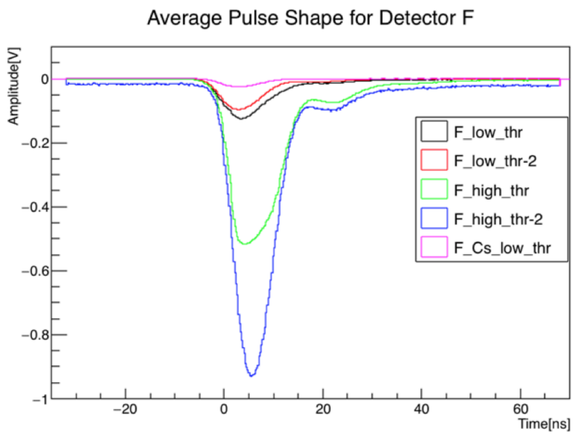

(b)

Figure 3: Pulse shapes collected by the oscilloscope. (a) Approximately 300 pulse shapes (black lines) and average one (red line). (b) Average pulse shape for each measurement.

3 Detector Characterization

3.1 Data taking

After that, I placed the experimental apparatus as shown in Figure 4, and recorded the signals by means of 14-bits flashADCs (FADC).

Figure 4: Experimental set-up: the two detectors are facing the radioactive source. I collected data for two detectors at the same time.

If the full scale of the FADC is not adequate, some signals would be saturated. Since the PSA routine would reconstruct the saturated signals as good, we should exclude them a posteriori: as can be seen in Figure 5, excluding events with an amplitude larger than 55000 channels will clean the spectra.

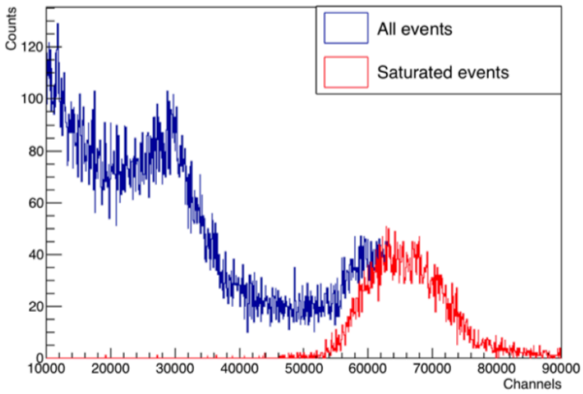

Figure 5: Energy spectrum taken by detector F. Blue line is all events recorded by the DAQ, and red line shows saturated events. Even though the precision of the FADC is 14-bits, the events are recorded as 16-bits data.

3.2 Energy calibration

I calibrated the relation between the deposited energy and the pulse height of the signal from each detector. I used gamma-ray sources: ^{137}Cs (661.7keV), ^{88}Y (898keV and 1836keV), $^{241}Am/Be$ (4.43MeV), and $^{244}Cm/C$ (6.13MeV). The peak corresponding to the Compton edge is broadened by the resolution of the detector, so the fitting function is the gaussian:

$$y = Ae^{-\frac{(x-\mu)^2}{2\sigma^2}} \tag{1}$$

where A, μ, and σ are the amplitude, mean and standard deviation of the distribution, respectively.

To be independent from the number of channels, we should convert the pulse height in mV. Assuming that the full scale of 16 bits FADC is A-[V], we can calculate the pulse height as the following:

$$A[V] : 2^{16}[ch] = PH[V] : PH[ch] \tag{2}$$

$$PH[V] = \frac{A[V] \cdot PH[ch]}{2^{16}} \tag{3}$$

The channel to energy calibration can be studied as the relation between the energy deposited in the detector (i.e. the Compton edge) and the pulse height of the signal in mV, as shown in Figure 6. The function to fit this plot is a linear function: $y = A + Bx$.

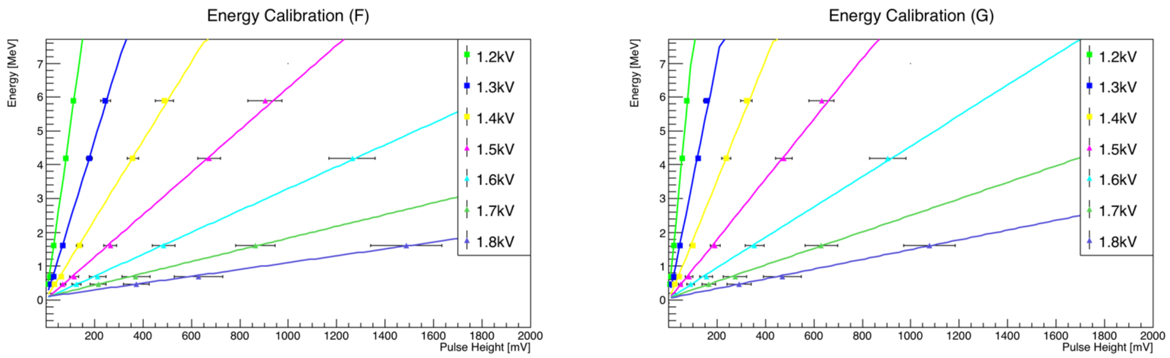

(a) $L_6D_6 - F$ (b) $L_6D_6 - G$

Figure 6: Relation between energy and pulse height.

The constants are shown in Table 2.

	$L_6D_6 - F$		$L_6D_6 - G$	
HV	A	B	A	B
1.2kV	0.05 ± 0.07	$(5.1 \pm 0.3) \times 10^{-2}$	0.01 ± 0.08	$(7.7 \pm 0.4) \times 10^{-2}$
1.3kV	0.05 ± 0.07	$(2.3 \pm 0.1) \times 10^{-2}$	-0.00 ± 0.08	$(3.6 \pm 0.2) \times 10^{-2}$
1.4kV	0.05 ± 0.07	$(1.17 \pm 0.06) \times 10^{-2}$	-0.01 ± 0.08	$(1.8 \pm 0.1) \times 10^{-2}$
1.5kV	0.02 ± 0.07	$(6.3 \pm 0.4) \times 10^{-3}$	0.02 ± 0.08	$(8.9 \pm 0.5) \times 10^{-3}$
1.6kV	0.06 ± 0.07	$(3.2 \pm 0.2) \times 10^{-3}$	0.05 ± 0.09	$(4.5 \pm 0.4) \times 10^{-3}$
1.7kV	0.09 ± 0.09	$(1.7 \pm 0.2) \times 10^{-3}$	0.1 ± 0.1	$(2.4 \pm 0.4) \times 10^{-3}$
1.8kV	0.09 ± 0.09	$(1.0 \pm 0.1) \times 10^{-3}$	0.1 ± 0.1	$(1.4 \pm 0.2) \times 10^{-3}$

Table 2: Fitting constants.

Here I define the deviation D from the linear behaviour as

$$D \equiv \frac{y - y_i}{y} = \frac{(A + Bx_i) - y_i}{A + Bx_i} \tag{4}$$

x_i *and* y_i are the pulse height in mV and the deposited energy in MeV, respectively. The deviation for each measurement was within ±8%.

3.3 Detector gain

The function of a gain curve for a photomultiplier is expressed as

$$Gain = A \cdot V^{n \cdot B} \tag{5}$$

where A and B are constants, V is the voltage applied to the photomultiplier and n is the number of dynodes in the photomultiplier. The photomultiplier used in the L_6D_6 detectors are the 9829QB

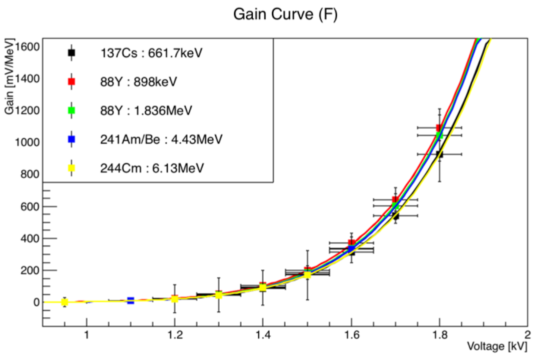

(a)

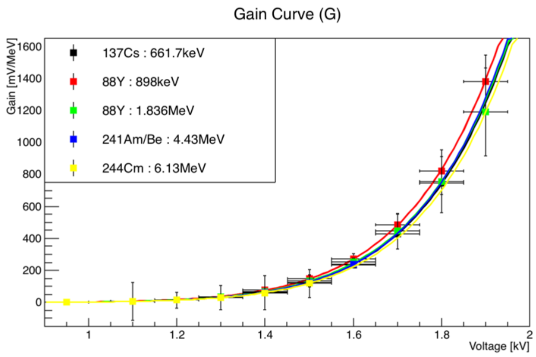

(b)

Figure 7: Fitting the gain curve for detector F (a) and G (b).

ET Enterprises, which have 12 dynodes. The constant B is dependent only of the material used in a photomultiplier, so it should be the same for every measurement.

Figure 7 shows the gain curve for each detector, while in Table 3 the values of the fitting constants are reported.

	$L_6D_6 - F$		$L_6D_6 - G$	
Source : Energy	A	B	A	B
^{137}Cs : 661.7keV	3.7 ± 1.6	0.78 ± 0.08	2.6 ± 1.1	0.80 ± 0.08
^{88}Y : 898keV	4.5 ± 1.7	0.78 ± 0.07	3.1 ± 1.2	0.79 ± 0.07
^{88}Y : 1836keV	3.8 ± 1.4	0.80 ± 0.07	2.8 ± 1.0	0.80 ± 0.06
$^{241}Am/Be$: 4.43MeV	2.6 ± 1.2	0.80 ± 0.08	2.4 ± 0.8	0.81 ± 0.08
$^{244}Cm/C$: 6.13MeV	4.0 ± 1.7	0.77 ± 0.96	2.3 ± 1.0	0.81 ± 0.96

Table 3: Constants of the gain curves.

4 Summary

I filled two L_6D_6 detectors with C_6D_6 scintillation liquid. After checking that the detectors are working, I extracted the average pulse shapes, which are necessary to apply the pulse shape analysis routine to analyze the raw data. I then made the plot which shows the relation between the energy deposited and the pulse height of the signal from each detector. From the width of broadened Compton edge, I calculated the energy resolution for each detector. Finally, I saw the gain curve for each detector and source, and confirmed that the fitting constants are behaving as expected.

Reference

[1]P.F. Mastinu et al., *New C_6D_6 detectors: reduced neutron sensitivity and improved safety*, n_TOF Internal Report, 2013